Journal of Power Sources 193 (2009) 146–149

Contents lists available at ScienceDirect

Journal of Power Sources

journal homepage: www.elsevier.com/locate/jpowsour

Short communication

Synthesis and characterization of ceria based nanometric powders

B. Matovic[a,*], Z. Dohcevic-Mitrovic[b], M. Radovic[b], Z. Brankovic[c], G. Brankovic[c], S. Boskovic[a], Z.V. Popovic[b]

[a] Institute of Nuclear Sciences "Vinca," 11001 Belgrade, Serbia
[b] Institute of Physics, Pregrevica, 11080 Belgrade, Serbia
[c] Institute for Multidisciplinary Research, Kneza Viseslava 1a, 11000 Belgrade, Serbia

ARTICLE INFO

Article history:
Received 5 January 2009
Received in revised form 11 March 2009
Accepted 12 March 2009
Available online 2 April 2009

Keywords:
Ceria solid solution
Raman spectroscopy
XRD measurements
Impedance spectroscopy

ABSTRACT

Nanopowdered solid solution $Ce_{1-x}Fe_xO_{2-\delta}$ samples ($0 \le x \le 0.1$) were synthesized by a self-propagating room temperature synthesis (SPRT). XRD and Raman spectroscopy at room temperature were used to study the vibrational properties of these materials as well as the Fe solubility in ceria lattice. Results show that all obtained powders are solid solutions with a fluorite-type crystal structure and all powders were nanometric in size. The average size of $Ce_{1-x}Fe_xO_{2-\delta}$ particles lies about 5 nm. The results of electrical properties of the sintered samples investigated by an ac impedance spectroscopy are also presented and discussed. It was confirmed that Fe^{3+} doped ceria material has a potential as electrolyte for intermediate-temperature solid oxide fuel cell applications.

1. Introduction

Ceria based materials have become one of the most important ceramic materials. There are a number of important uses such as automobile exhaust catalyst, as an ionic conductor, as a gas sensor, as an electrolyte material for solid oxide fuel cells (SOFC), as mechanical polishing medium and as additive to other high-tech ceramics [1–4]. Especially ceria solid solution has been acknowledged to be most promising electrolyte for intermediate temperature (500–700 °C) fuel cells. For comparable doping conditions, the overall oxygen ionic conductivity in doped ceria is approximately an order of magnitude greater than that of conventional yttrium stabilized zirconia [5]. The larger ionic radius of Ce^{4+} (0.97 Å) than Zr^{4+} (0.72 Å), results in much more open structure through which oxygen ions can easily migrate [6]. This allows ceria to be used as an electrolyte at moderate operating temperatures. The key factor in the design of modified ceria is the choice of dopant elements, as well as their amount introduced. In addition, the preparation method of the powder has also very strong influence on the homogeneity and stability of the solid solutions.

Conventional solid state reaction method involves mixing of corresponding oxides and heating them at elevated temperatures for extended duration [7–9]. However, very low diffusion coefficients of ions in solid reactions requires intermittent grinding and repeated heating and grinding for extended period of time to form the desired single-phase compound. On the other side, high temperature treatment usually results in large crystal grow and hence low surface area. Moreover, the conductivity in nanocrystalline grain boundary regions is greater than for longer grains [10]. In this respect it is important to develop powders of high quality with particle size in the nanometric range.

One of the methods that are cost and time effective is the self-propagating room temperature (SPRT) synthesis of powders. SPRT procedure is based on the self-propagating room temperature reaction between metal nitrates and sodium hydroxide. This reaction is spontaneous and terminates extremely fast [11,12].

Nanosized doped ceria with oxides of di- or trivalent metals are shown to be a promising solid electrolyte with good ionic conductivity at low temperature. Namely, partial replacement of Ce^{4+} ions with di- or trivalent ions produces a large density of oxygen vacancies in ceria lattice enhancing the conductivity of these materials [13,14]. The ionic conductivities of ceria ceramics doped with various ions (Ca^{2+}, Sr^{2+}, Ba^{2+}, Y^{3+}, Ln^{3+}, Sm^{3+}, Gd^{3+}, Nd^{3+}) at different concentrations have been extensively investigated. Among all these dopants, Sm^{3+} and Gd^{3+} are found to produce the highest conductivity [15,16].

From the point of view of cost reduction, samarium and gadolinium as the dopants would cause higher material expense. The use of an inexpensive dopant with acceptable electrochemical properties is more preferable. A good candidate may be iron, because of its lower valence state than ceria and low price. Also, there is lack of literature data about iron as a dopant ion in ceria solid solution.

* Corresponding author. Tel.: +381 11 2439 454; fax: +381 11 2439 454.
E-mail address: mato@vin.bg.ac.yu (B. Matovic).

0378-7753/$ – see front matter © 2009 Elsevier B.V. All rights reserved.
doi:10.1016/j.jpowsour.2009.03.053

Therefore, in the present study, we report a SPRT method for preparation of nanocrystalline powders of ceria and Fe-doped ceria. Also in order to develop a new electrolyte for intermediate temperature SOFC, the ionic conductivity for some composition of Fe-doped ceria was studied.

2. Experiment

For experimental work cerium and iron nitrates were used in the reaction with sodium hydroxide. The used nitrates were p.a. (pro analyze) compound (Aldrich, Germany) and all in the form of hexahydrates. The compositions of the starting reacting mixtures were calculated according to the nominal composition of the final reaction product. Ceria doped powders were synthesized by SPRT methods according to reaction:

$$2\cdot[(1-x)(Ce(NO_3)_3\cdot 6H_2O)+x(Fe(NO_3)_3\cdot 6H_2O)] + 6NaOH + (1/2-\delta)O_2 \rightarrow 2Ce_{1-x}Fe_xO_{2-\delta} + 6NaNO_3 + 15H_2O$$

The following compositions were prepared: CeO_2, $Ce_{0.99}Fe_{0.01}O_{2-\delta}$, $Ce_{0.97}Fe_{0.03}O_{2-\delta}$, $Ce_{0.95}Fe_{0.05}O_{2-\delta}$, $Ce_{0.925}Fe_{0.075}O_{2-\delta}$ and $Ce_{0.90}Fe_{0.10}O_{2-\delta}$. During SPRT synthesis hand-mixing of nitrates with NaOH was performed in alumina mortar for ~10 min until the mixture got light brown. After being exposed to air for 4 h, the mixture was suspended in water. Rinsing out of $NaNO_3$ was performed in centrifuge—Centurion 1020D, at 3500 rpm for 10 min. This procedure was repeated three times with distilled water and twice with ethanol [11].

The powders were pressed uniaxial without any binder at 100 MPa into pellets using a die 10 mm in diameter, followed by isostatic pressuring at 200 MPa. The samples were sintered in a furnace at 1300 °C for 4 h in static air.

Powder XRD patterns of all the powders and samples heat treated at different temperatures were recorded on Siemens X-ray Diffractometer (Kristaloflex 500) with Ni filtered Cu K_α radiation and using Si as an external standard. The measurements were performed in the 2θ range from 20° to 80° in a continuous scan mode with a step width of 0.02° and at a scan rate of 1° 2θ min^{-1}. The average crystallite size (D), was calculated from Scherrer's formula: $D = 0.9\alpha/\beta\cos\theta$, where α is the wavelengths of the X-rays, θ is diffraction angle, $\beta = (\beta_m^2 - \beta_s^2)$, β is corrected half-width, β_m observed half-width and β_s is half-width of the standard Si sample (provided by Siemens Company).

Unpolarized micro-Raman scattering measurements were performed in the backscattering configuration using Jobin Yvon T64000 Spectrometer equipped with nitrogen cooled Symphony® charge-coupled-device detector (CCD). As an excitation source we used 514.5-nm line of Ar-ion laser operating at low power ~10 mW in order to avoid sample heating.

Impedance spectra of the investigated samples were taken in temperature interval from 200 to 600 °C and in frequency range from 100 Hz to 1 MHz (HP4194A Impedance/Gain Phase Analyzer). The signal level was 1 Vrms. Silver painted electrodes were used for the impedance measurements.

3. Results and discussion

It is well known that that the solubility of Fe^{3+} into ceria compound is very small (less than 1.0 at.%) in the range from room temperature to 1500 °C [17,18]. However, according to X-ray powder diffraction analysis, the obtained powders are single phase, independent of dopant concentration in the range investigated (Fig. 1). Peaks related to isolated Fe-phases are not observed and all of solid solution powders exhibit the fluorite crystal structure. This high solubility may be attributed to nanometric nature of powders. XRD analysis reveals that all peaks for each sample were significantly broadened indicating small crystallite size and/or strain. It exhibits very diffuse diffraction lines, in such way that some atomic planes are impossible to indicate (*hkl*: 200, 400, 311, 420).

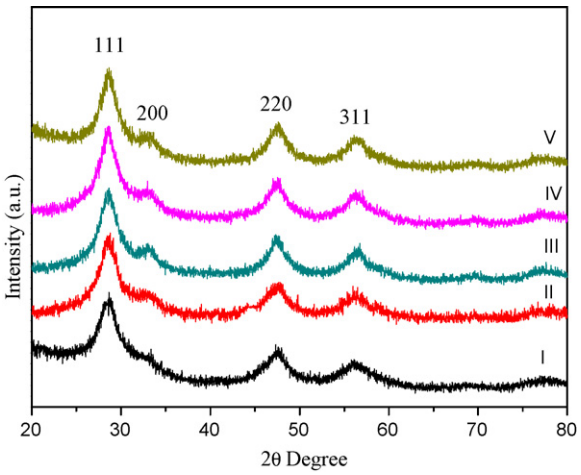

Fig. 1. X-ray diffraction patterns of $Ce_{1-x}Fe_xO_{2-\delta}$ powders (I: $x = 0$, II: $x = 0.03$, III: $x = 0.05$, IV: $x = 0.075$ and V: $x = 0.1$).

Cell parameters calculation on the basis of X-ray results (Fig. 2), shows the linear dependence versus atomic percentage, x, of Fe^{3+} ions. With increasing of Fe ion concentration the cubic ceria lattice shrinks. According to Shannon's compilation [11], the ionic radii of Ce^{4+} and Fe^{3+} for CN 8, are 0.97 and 0.78 Å, respectively. Thus, doping with a smaller sized Fe^{3+} ions and increasing dopant concentration will keep on reducing cell lattice. Also, lattice parameter (a_o) of doped ceria versus Fe^{3+} content, obeys Vegard's law. The crystallite size, calculated on the basis of XRD data, for all powders lay below 5 nm.

On the other side, annealed powders exhibit sharpened diffraction lines resulting from increasing the crystallite size. Powders annealed at 1300 °C are well crystallized. The XRD patterns for all compositions match very well with cubic fluorite form of CeO_2, which implies that solid solutions obtained with SPRT method can maintain at high temperature and that are very stable in high temperature. However, several weak diffraction lines of unknown phase are present in sintered sample doped with 7.5% of Fe, indicating that the limit of solubility of Fe in CeO_2 is in the range of 5–7.5 wt.% at 1300 °C (Fig. 3). This trace of unknown phase suggests that segregation of some amount of iron oxide at CeO_2 grain boundaries occurred at high temperature.

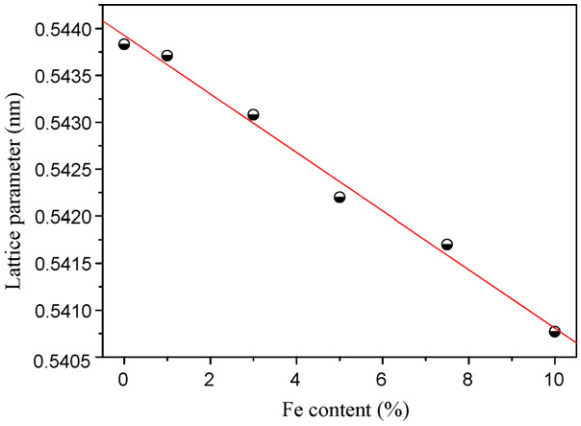

Fig. 2. Lattice parameter (a_o) of doped ceria as a function of Fe content in samples ($Ce_{1-x}Fe_xO_{2-\delta}$).

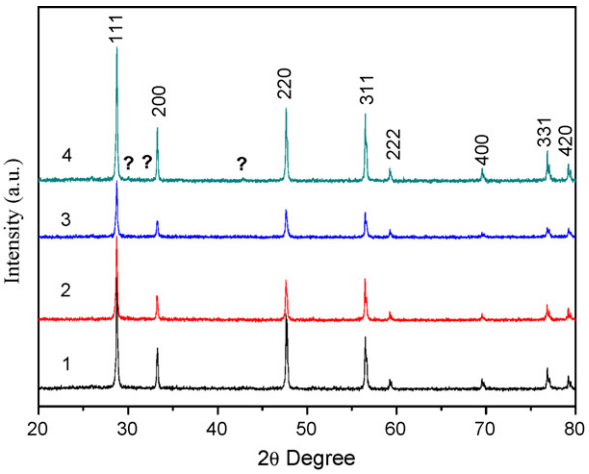

Fig. 3. X-ray diffraction patterns of $Ce_{1-x}Fe_xO_{2-\delta}$ powders heat treated at 1300 °C for 4 h (1: $x = 0.01$, 2: $x = 0.03$, 3: $x = 0.05$, 4: $x = 0.075$). ? trace of unknown phase.

Raman spectra confirm the XRD analysis. Fig. 4 shows Raman spectra of $Ce_{1-x}Fe_xO_{2-\delta}$ ($0.01 < x < 0.075$) samples before (open circles) and after (solid gray line) sintering at 1300 °C. Main feature of the first order Raman spectrum of CeO_2 is a F_{2g} mode located at 465 cm^{-1} in the bulk sample. In nanosized $Ce_{1-x}Fe_xO_{2-\delta}$ samples this mode is shifted to lower energies (451 cm^{-1}), with increased linewidth and pronounced asymmetry at low energy side. Nanosized effects like phonon confinement, strain and nonstoichiometry can contribute to the observed changes in Raman peak profile [19]. To explain properly the evident phonon softening and increased asymmetry of the F_{2g} mode we have used the phonon confinement model (PCM) that incorporates particle size and strain effects [20]. Raman intensity is calculated over the entire Brillouin zone by the following relation:

$$I(\omega) = \sum_{1}^{3} \int_0^\infty \rho(L)\mathrm{d}L \int_{BZ} \frac{\exp(-(q^2L^2/8\beta))}{[\omega - (\omega_i(q) + \Delta\omega_i(q,L))]^2 + [\Gamma_0/2]^2} d^3q$$

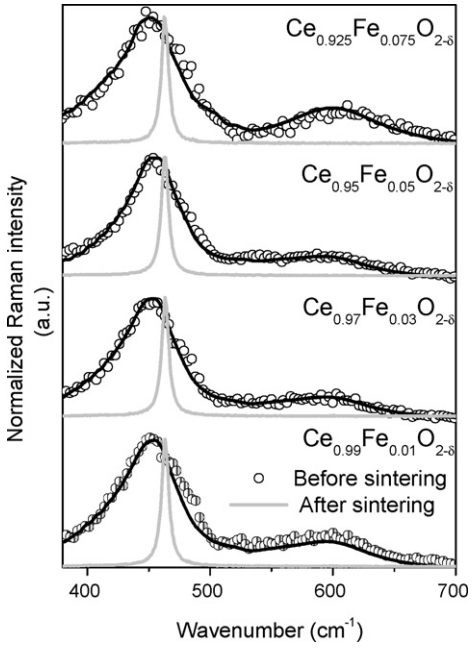

Fig. 4. Raman spectra of $Ce_{1-x}Fe_xO_{2-\delta}$ ($0.01 < x < 0.075$) samples before (open circles) and after (solid gray line) sintering at 1300 °C together with fit (solid black line) according to PCM.

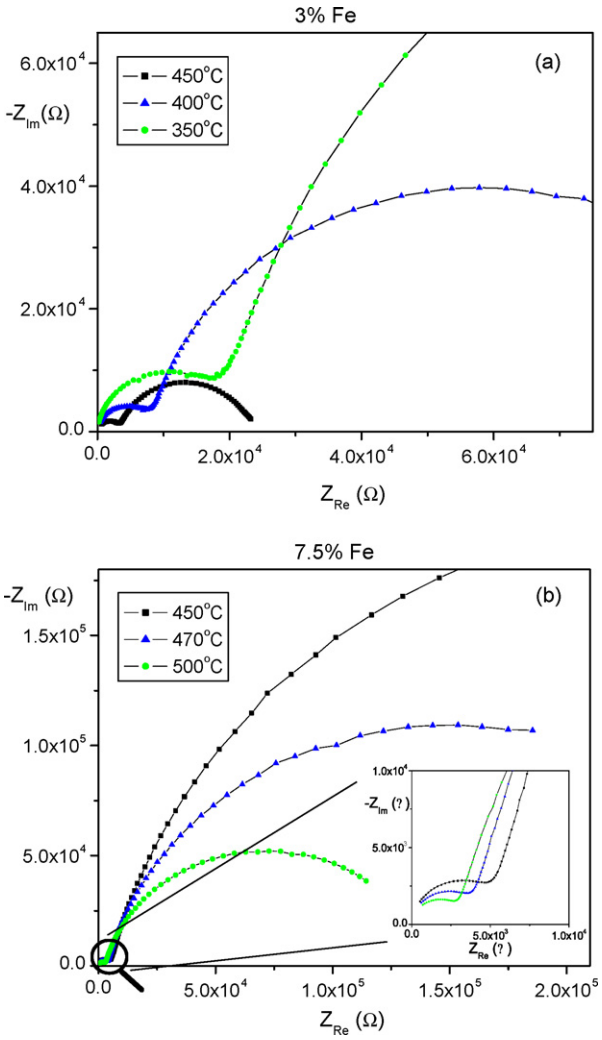

Fig. 5. Impedance spectra of samples with 3% Fe (a) and 7.5% Fe (b).

where L is particle size and $\rho(L)$ is Gaussian particle size distribution. The phonon dispersion of F_{2g} mode is represented by parabolic fits to phonon dispersion curves for CeO_2 and the effect of strain is included through $\Delta\omega_i(q,L)$ term [19]. Factor β is an adjustable parameter depending on the strength of the phonon confinement and Γ_0 is the natural linewidth of F_{2g} mode. The calculated spectra (solid black line) using the strong confinement condition ($\beta \sim 4\pi^2$) together with experimental data (open circles) is presented in Fig. 4. The best agreement between theoretical curve and experimental results is obtained for the average particle size of $L_0 = 6.5$ nm.

After sintering Raman mode is shifted to higher frequencies, 464 cm^{-1}, its linewidth is reduced down to 9 cm^{-1} and becomes totally symmetric. These values correspond to values of bulk CeO_2 [19] which confirm that our sample has transformed from nano- to polycrystalline during sintering.

Beside the first order Raman mode additional band at 600 cm^{-1} appears in the Raman spectrum of samples taken before sintering. This mode can be attributed to intrinsic oxygen vacancies generated in ceria lattice due to nonstoichiometry of nanopowders.

Table 1
Activation energies of conduction for grain (E_g) and grain boundary (E_{gb}).

Sample	E_g (eV)	E_{gb} (eV)
$Ce_{0.97}Fe_{0.03}O_{2-\delta}$	0.644 ± 0.007	0.94 ± 0.02
$Ce_{0.925}Fe_{0.075}O_{2-\delta}$	0.600 ± 0.006	1.15 ± 0.03

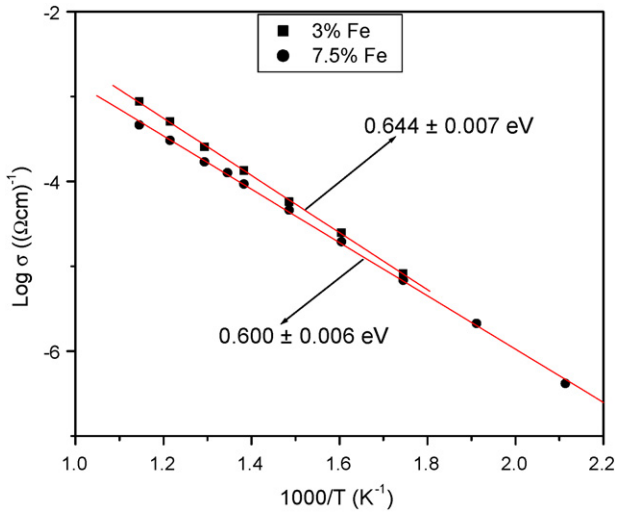

Fig. 6. Arrhenius plots ionic conductivities of samples with 3% Fe and 7.5% Fe.

During sintering, surface to volume ratio of nanoparticles changes and mode of intrinsic oxygen vacancies gradually decrease in intensity until it totally vanishes from Raman spectra as a consequence of approaching stoichiometry of nanopowders.

Impedance spectra of the investigated samples were taken in temperature interval from 200 to 600 °C and in frequency range from 100 Hz to 1 MHz. Some of the spectra in the form of the Nyquist plots are given in Fig. 5. Two well-defined semicircles were clearly visible in all samples for almost all measuring temperatures. Conductivities were calculated from these spectra taking account samples dimensions (Fig. 6). Based on temperature dependence of conductivity activation energy for ionic conductivity and conductivity through grain boundary were determined (Table 1). It was found that the ionic grain conductivity decreases with increase in Fe^{3+} content. For example σ_g of the sample with 3% of Fe^{3+} and 7.5% of Fe^{3+} measured at 500 °C were 2.54×10^{-4} and 1.70×10^{-4} S cm^{-1}, respectively. At higher temperatures this difference was more pronounced. Conductivities of grain boundary regions also decreased with increase in dopant content together with corresponding activation energies. The higher resistance of the samples with higher concentration of Fe^{3+} could be explained by segregation of some amount of Fe oxide at CeO_2 grain boundaries. Since there is no literature data for electrical properties of CeO_2 doped with Fe^{3+}, these results could be compared with some other systems in which the trivalent cations were used as dopants for CeO_2. For example it was reported on conductivities and activation energies of conduction in samples doped with Sb^{3+}, Sm^{3+}, Al^{3+}, Bi^{3+}, Ga^{3+} and In^{3+} [21]. In comparison to these systems we obtained higher values of conductivities. Values of $\log \sigma_g$ reported in reference [21] were from −6.87 to −9.50, at 200 °C, depending on dopant used. At the same temperature we obtained $\log \sigma_g$ −6.38 in sample with 7.5% of Fe^{3+}. At the same time we obtained significantly lower values of activation energies. In comparison with some other literature data on CeO_2 doped for example with Gd [22] our values were for the order of magnitude lower (reported σ_g about 3×10^{-4} S cm^{-1} at 350 °C) and at the same temperature the highest conductivity that we measured in our samples was 2.49×10^{-5} S cm^{-1}.

Generally, conductivity results showed that although it is possible to achieve high solubility of Fe^{3+} in CeO_2 using SPRT method, such high concentration of dopant does not further increase conductivity. Therefore, further optimization of dopant concentration based on electrical measurements should be done to obtain optimal electrical and other properties.

4. Conclusions

In summary, $Ce_{1-x}Fe_xO_{2-\delta}$ solid solutions ($0.01 \leq x \leq 0.10$) were prepared by low cost SPRT method that is easy to handle. It was found that the ceria powders with Fe dopant up to 10% are solid solution with fluorite structure. Particle size lies in the nanometric range (5 nm). The Raman spectra for all dopant concentrations are well described using a spatial correlation model with combined size and inhomogeneous strain effects. Impedance spectroscopy reveals that the ionic grain conductivity slightly decreases with increase in Fe^{3+} content. Grain conductivities (σ_g) of the sample with 3% of Fe^{3+} and 7.5% of Fe^{3+} measured at 500 °C were 2.54×10^{-4} and 1.70×10^{-4} S cm^{-1}, respectively. Nevertheless, we believe that we can further improve electrical properties of our samples by optimization of composition and processing conditions.

Acknowledgement

This project was financially supported by the Ministry of Science of Serbia (projects numbers: 142003 and 142040).

References

[1] A. Trovarelli, C. de Leiterburg, M. Boaro, G. Dolcetti, Catal. Today 50 (1999) 353–367.
[2] D. Waller, J.A. Lane, B.C.H. Steele, Solid State Ionics 86 (1996) 767–772.
[3] T. Suratwala, R. Steele, M.D. Feit, L. Wong, P. Miller, J. Menapace, P. Davis, J. Non-Crystalline Solids 354 (2008) 2023–2037.
[4] A. Tsoga, A. Gupta, A. Naoumidis, P. Nikolopoulos, Acta Mater. 48 (2000) 4709–4714.
[5] B.C.H. Steele, Solid State Ionics 129 (2000) 95–110.
[6] S.M. Haile, Acta Mater. 51 (2003) 5981–6000.
[7] S.E. Dann, Reactions and Characterization of Solids, Wiley, New York, 2000, pp. 141–148.
[8] S. Wang, K. Maeda, M. Awano, J. Am. Ceram. Soc. 85 (2002) 1750–1753.
[9] A.R. West, Solid State Chemistry and its Applications, Wiley, New York, 1991, pp. 36–64.
[10] M. Oljaca, R. Maric, S. Shanmunghan, A. Hunt, Am. Ceram. Soc. Bull. 82 (2003) 38–47.
[11] S. Boskovic, D. Djurovic, Z. Dohcevic-Mitrovic, Z.V. Popovic, M. Zinkevich, F. Aldinger, J. Power Sources 145 (2005) 237–242.
[12] S. Boskovic, S. Zec, M. Ninic, J. Dukic, B. Matovic, D. Djurovic, F. Aldinger, J. Optoelect. Adv. Mater. 10 (2008) 515–519.
[13] C. Peng, Y. Wang, K. Jiang, B.Q. Bin, H.W.V. Liang, J. Feng, J. Meng, J. Alloys. Compd. 349 (2003) 273–278.
[14] A. Sin, Y. Dubitsky, A. Zaopo, A.S. Arico, L. Gullo, D. La Rosa, S. Siracusano, V. Antonucci, C. Oliva, O. Ballabio, Solid State Ionics 175 (2004) 361–366.
[15] J.A. Kilner, Solid State Ionics 8 (1983) 201–207.
[16] R. Gerhard-Anderson, A.S. Nowick, Solid State Ionics 5 (1981) 547–550.
[17] T. Zhang, P. Hing, H. Huang, J. Kilner, J. Eur. Ceram. Sci. 21 (2001) 2221–2228.
[18] T. Zhang, P. Hing, H. Huang, J. Kilner, J. Mater. Proc. Technol. 113 (2001) 463–468.
[19] E. Spanier, R.D. Robinson, F. Zhang, S.W. Chan, I.P. Herman, Phys. Rev. B 64 (2001) 245407–245408.
[20] Z.D. Dohčević-Mitrović, M.J. Šćepanović, M.U. Grujić-Brojčin, Z.V. Popović, S.B. Bošković, B.M. Matović, M.V. Zinkevich, F. Aldinger, Solid State Commun. 137 (2006) 387–390.
[21] H. Zhang, J. Wang, S.-C. Wang, Z.-C. Li, Trans. Nonferrous Met. Soc. China 17 (2007) s565–s569.
[22] T.S. Zhang, J. Ma, Y.J. Leng, S.H. Chan, P. Hing, J.A. Kilner, Solid State Ionics 168 (2004) 187–195.